RESEARCH ARTICLE

Preparation, Characterization and Evaluation of Monosaccharide Tagged Nanostructured Lipid Carriers for Targeting of Etravirine to Macrophagic AIDS Viral Reservoirs

Bala Tripura Sundari[1*], CVS Subramanyam[2]

[1]*Faculty of Pharmacy, College of Technology, Osmania University, Hyderabad, Telangana, India.*
[2]*Department of Pharmaceutics Gokaraju Rangaraju College of Pharmacy, Hyderabad, Telangana, India.*

Received: 12th March, 2024; Revised: 03rd May, 2024; Accepted: 2nd August, 2024; Available Online: 25th September, 2024

ABSTRACT

Purpose of the study: The present study aimed to develop and examine monosaccharide-decorated nanoparticles specifically designed for macrophage targeting of etravirine.

Methods: Nanostructured lipid carriers (NLC) were prepared with stearylamine as such or after tagging with mannose and galactose as one of the lipid components of NLC. Prior to synthesis, a docking study was used to analyze the potential for interaction of the stearylamine- sugar conjugates with respective lectin receptors. Mannose and galactose-conjugated stearylamine were separately synthesized. Fourier-transform infrared spectroscopy (FTIR), mass spectrometry (MS) and nuclear magnetic resonance (NMR) studies were used to assess successful reactions. Etravirine-loaded non-targeted nanostructured lipid carriers (NLCs) were synthesized with the emulsification solvent evaporation method and characterized for parameters such as zeta potential, *in-vitro* release, entrapment efficiency and particle size.

To create targeted nanoparticles, stearylamine was replaced with either of the conjugated lipids in the formulation. For stability, all NLC dispersions were lyophilized. *In-vitro* investigations included cellular uptake and cytotoxicity assessments in the RAW 264.7 macrophage cell line. Following intravenous administration of the NLCs in Wistar rats, *in-vivo* biodistribution was evaluated.

Results: The docking studies showed good binding potential of both conjugated lipids for respective receptors. Evaluation of synthesized products showed successful conjugation of sugars to stearylamine. The synthesized nanoparticles demonstrated impressive etravirine loading capabilities and exhibited a circular shape with a mean size of approximately 260 nm. Drug release from all NLC formulations persisted for over 24 hours and remained stable after lyophilization. *In-vitro* evaluations in the RAW 264.7 macrophage cell line revealed that mannosylated nanoparticles had enhanced uptake when compared to non-targeted and galactosylated counterparts. *In-vivo* plasma and tissue distribution studies corroborated the *in-vitro* findings, as the mannosylated NLCs displayed a higher distribution into organs with a rich presence of macrophages.

Conclusion: The studies indicate that while sugar tagging of nanoparticles can prove to be an effective strategy for targeting drugs to macrophagic tissue for tackling latent AIDS virus, the choice of sugar is critical.

Keywords: Mannose, Galactose, Mannosylated stearylamine conjugate, Galactosylated stearylamine conjugate, Etravirine, Macrophage targeting.

International Journal of Drug Delivery Technology (2024); DOI: 10.25258/ijddt.14.3.05

How to cite this article: Sundari BT, Subramanyam CVS. Preparation, Characterization and Evaluation of Monosaccharide Tagged Nanostructured Lipid Carriers for Targeting of Etravirine to Macrophagic AIDS Viral Reservoirs. International Journal of Drug Delivery Technology. 2024;14(3):1278-1291.

Source of support: Nil.

Conflict of interest: None

INTRODUCTION

Macrophages constitute one of the most important viral reservoirs along with CD4+ cells in human immunodeficiency virus (HIV) infections[1]. As the virus predominantly resides in macrophages within organs like the liver, spleen, and mononuclear phagocytic system, they serve as significant reservoirs, underscoring the need for the development of drug formulations specifically targeting macrophages to inhibit HIV replication. Various carrier systems, including liposomes[2], microspheres[3], and nanoparticles[4], have been extensively studied for macrophage targeting. Among these, nanoparticles offer distinct advantages, such as enhanced accumulation in

**Author for Correspondence: balasvcp@gmail.com*

macrophage-rich organs. Leveraging nanoparticles as carriers may facilitate selective drug delivery to infected cells, reducing required dosages, minimizing dose-dependent side effects, and sustaining drug release.

Nanocarriers are one such versatile drug delivery system, which may be used for the delivery of antiretroviral drugs due to their ability to target the drug to specific cells or intracellular compartments due to their size. They could be engineered either by passive or ligand-mediated targeting mechanisms.

Engineered nanoparticles, in particular, exhibit superior accumulation in macrophage-rich organs, making them promising candidates for targeted delivery of antiviral agents to macrophages. Notably, macrophages feature receptors for molecules like folic acid, mannose, and galactose[5,6] on their surface, aiding in recognition and endocytosis processes. Consequently, macrophages exhibit enhanced phagocytosis of carriers bearing ligands such as mannose, galactose, and folic acid compared to those lacking such ligands[7].

Treatment with etravirine (ETR) is particularly noteworthy due to its effectiveness against NNRTI-resistant strains of the virus[8]. However, oral administration of ETR faces challenges such as poor permeability, limited bioavailability, and low water solubility primarily due to its highly hydrophobic nature. To overcome these obstacles, ETR-loaded nanoparticles can be employed through parenteral administration. This method not only overcomes the limitations associated with oral bioavailability but also allows for targeted delivery to cellular hosts utilized by HIV for replication, ultimately enhancing the therapeutic impact.

This study aims to develop lipidic nanoparticles loaded with etravirine, with a focus on targeting cellular reservoirs of HIV, such as macrophages. To achieve this, mannose and galactose are employed as targeting ligands. The incorporation of these ligands is intended to boost macrophage uptake, facilitating greater distribution of the drug to organs known to serve as major reservoirs for HIV.

MATERIALS AND METHODS

Etravirine (ETR) was generously provided by Hetero Pharma, a company based in Hyderabad, India. Mannose and galactose were procured from Sisco Research Laboratories Pvt. Ltd, a firm located in Maharashtra. Capryol 90®, Labrafac®, and Labrasol® were graciously supplied as gift samples by Gattefosse, a company headquartered in Mumbai, India. Tween 20 & 80, Poloxamer (188 and 407) were obtained from Sigma Aldrich, a well-known supplier. Dichloromethane was sourced from SD Fine Chemicals Limited, a company based in Mumbai, India. Qualikems Fine Chemicals Pvt Ltd, a firm situated in Vadodara, India has supplied Polyvinyl alcohol (with a degree of polymerization of 1700-1800). Stearylamine was procured from SRL Chemicals, a company based in Maharashtra, India, while glyceryl monostearate was obtained from RX Chemicals, also located in Maharashtra, India. Hi-Media Laboratories Pvt Ltd readily provided us with Dulbeco's Modified Eagle Medium (DMEM) and MTT. RAW cell lines were acquired from NCCS Pune.

Studies on molecular docking of mannose and galactose-conjugated lipid

To study the interaction between galactose and mannose receptors and their corresponding ligands, protein templates were obtained from the Protein Data Bank (PDB) with IDs 1JZN (galactose-specific C-type lectin receptor) and 1EGG (C-type carbohydrate domain recognition from mannose macrophage receptor). The ligands, D-galactose conjugated stearyl amine and D-mannose conjugated stearyl amine, were drawn with ChemBioDraw Ultra 14.0 (Cambridge Soft interface, PerkinElmer, Cambridge, Poland).

Autodock Vina, an automated docking program included with the PyRx 0.8 program (Scrips Research, La Jolla, CA, USA), was used for docking research. This tool facilitates the three-dimensional analysis of ligand-receptor binding. Binding energy scores are obtained from docking calculations and are useful in assessing the efficiency of the interaction. Using the BIOVIAL Discover Studio Visualizer v16.1.0.15350[9], the ideal ligand posture was further investigated for molecular orientation and interactions between amino acids.

Moreover, the Molinspiration web tool was utilized to evaluate the pharmacokinetic parameters of the synthesized lipids. This comprehensive assessment provides valuable insights into their properties and interactions, ensuring a thorough understanding of their behavior.

Synthesis of Stearylamine-Mannose (STMN) conjugate and Stearylamine-galactose (STGL) conjugate

The synthesis of stearylamine-sugar conjugates, specifically STMN (stearylamine-mannose) and STGL (stearylamine-galactose), was conducted with a well-established method with certain modifications.[10] To make STMN, 10 mL of ethanol and 5 mmol of stearylamine were combined in a round-bottom flask and warmed up to 70°C. After adding 5 mmol of D-mannose, the liquid was continuously whisked on a magnetic stirrer until all of the sugar had dissolved. The mixture was then stirred for a further two hrs at 70°C. Once all of the sugar had dissolved, the mixture was allowed to cool to 40°C before being diluted with 35 mL of hexane. After being collected at room temperature, the resultant crystals were cleaned with hexane and dried. The process for synthesizing STGL was the same; mannose was substituted with galactose. Once synthesized, both conjugates underwent further characterization to evaluate their physicochemical properties[11], ensuring comprehensive understanding and optimization of these compounds.

Characterization of STMN and STGL conjugates

After the synthesis, the products were analyzed for their percentage yield and melting point. Subsequently, they underwent spectroscopic studies to assess the success of the conjugation process.

FTIR Spectroscopy

The infrared absorption spectra of stearylamine, STMN and STGL were noted with the KBr disc method on a QSTAR XL CCMS FTIR-8400s.

H^1 NMR Spectroscopy

The Bruker Avance instrument II 500MH was used to determine the ^{1}H-NMR spectra of STMN and STGL. In relation to the internal standard tetramethyl silane (TMS), the values of the chemical shift are given in parts per million (ppm).

Mass Spectroscopy

Mass spectra of STMN and STGL were noted at room temperature on the Shimadzu mass spectrometer.

Preparation of ETR nanoparticles

Preparation of non-targeted nanoparticles

Conventional non-targeted nanostructured lipidic carriers of ETR (abbreviated as BNP) were prepared with solvent emulsification and evaporation techniques. Measured amounts of solid lipids stearylamine (27 mg), glyceryl monostearate (54 mg) and liquid lipid Capryol 90 (99 mg) along with 20 mg ETR were dissolved in 5 mL of dichloromethane. The external phase (40 mL of 1.5% PVA solution) was kept stirred at 2000 rpm with an overhead stirrer (Remi motors). During this time, the organic phase was slowly injected into it with the help of a syringe and needle over a period of 2 minutes with continuous stirring, resulting in emulsification. The crude dispersion was immediately subjected to probe sonication (Q Sonica Q55) for a period of 30 minutes at 80% amplitude. Next, the nano-dispersion produced was once again transferred to the overhead stirrer to allow for complete solvent evaporation. The entire procedure was conducted at 25ºC. The NLC dispersion was promptly subjected to evaluation studies. The resultant NLC dispersion was subjected to estimation of zeta potential, size, drug entrapment and *in-vitro* drug release prior to lyophilization[12].

Characterization of the NLC

Particle size and zeta potential

Zeta sizer from Malvern USA was used to examine the formulations' particle sizes and zeta potential. The samples were diluted with milli Q water, which has a viscosity of 0.887 cps and a refractive index of 1.40, in order to ensure an accurate assessment. The polydispersity index (PDI) and mean particle size for each formulation were found in this dilution. Moreover, the same device was used to assess the formulations' zeta potential, which offered vital information about the stability and any interactions between the particles in the formulations.

Scanning electron microscopy

The Hitachi S3700N scanning electron microscope was used to acquire SEM images for the nano-dispersion. Until the sample was ready for analysis, the dispersion was first applied to a sample stub and allowed to dry. This process maintained the dispersion's structural integrity and prevented any potential damage to the nanoparticles during imaging.

Following drying, a thin gold layer was sputtered onto the sample's surface to provide the conductive coating required for precise measurement in an extremely high vacuum. The gold coating enhanced the contrast and visibility of the nanoparticles within the dispersion, allowing for a more detailed examination of their morphology and distribution.

Entrapment efficiency

To determine the Entrapment efficiency of the developed ETR-NLC, the centrifugation method was employed. A 5 mL sample of the ETR-NLC dispersion was centrifuged with a Remi R-24 research centrifuge at 17,000 rpm for 1-hour. This process allowed for the separation of entrapped and non-entrapped ETR particles based on their density and size differences. After centrifugation, the dispersion medium was and then diluted with methanol to facilitate accurate analysis.

The ETR content in the diluted sample was determined using UV-Vis spectrophotometry at the ETR-specific wavelength of 311 nm. By comparing the absorbance values of the diluted sample to a calibration curve of known ETR concentrations, the exact quantity of ETR in the sample may be determined.

Finally, the entrapment efficiency was calculated with the following equation:

Entrapment Efficiency (%) = (Total amount of ETR - Amount of free ETR) / Total amount of ETR × 100

Drug Entrapment Efficiency (%w/w) = (W_{total}– W_{drug}) X 100/ W_{total}

Where W_{total} = Total amount of ETR used in the formulation

W_{drug} = Amount of ETR in supernatant

***In-vitro* Drug Release**

Dialysis bag method was used to examine the ETR release profile from the produced biodegradable nanoparticles (BNPs). For this, a dialysis membrane with a molecular weight cutoff of 12 to 14 kDa was acquired from Hi-Media, India. In two different dialysis bags, 2.5 mg of ETR was mixed with 2 mL of nanostructured lipid carrier (NLC) dispersion to start the release investigation. Using clips, the ends of the bags were tightly secured to prevent leaks throughout the experiment.

After that, each sealed dialysis bag was placed inside a beaker that held 50 mL of the release medium. The pH 7.4 phosphate-buffered saline (PBS) and 1% w/v Tween 80, which mimics the physiological environment and aids in maintaining sink conditions, made up the release medium. The beaker was set up on a magnetic stirrer with a stirring bar to guarantee even temperature and effective mixing, and the study's temperature was kept constant at 37ºC.

About 2 mL aliquots were cautiously removed from the release medium for examination at prearranged intervals. UV-vis spectrophotometry was used to measure the concentration of ETR in the samples at a wavelength specific to the ETR molecule, 311 nm. The concentration of ETR in the samples was then found using the acquired absorbance values.

After every withdrawal, the same volume of new release medium was introduced to maintain a steady volume of the release medium and guarantee precise computations. Throughout the course of the study, this procedure was repeated numerous times to acquire the cumulative release profile of ETR from the BNPs.

Lyophilization

To prepare the drug-loaded NLC (BNP) for long-term storage and stability, lyophilization was performed with mannitol as a cryoprotectant.[13] In this process, 9% w/v mannitol was incorporated into the total volume of the NLC dispersion to be lyophilized. The mannitol acts as a stabilizer and protects the NLC structure during the freezing and drying process.

Martin Christ Alpha 1-2 LD plus lyophilizer was used to carry out the lyophilization, or freeze-drying, process. There are three key stages to the process: freezing, primary drying, and secondary drying. To create ice crystals, the NLC dispersion was cooled to -55°C during the freezing stage. This stage facilitates the solvent's extraction from the frozen sample.

In the primary dying step, the temperature in the lyophilizer chamber was enhanced, and the pressure was reduced to allow the sublimation of ice crystals directly from the solid phase to the gas phase, leaving the mannitol and NLC behind as solid residue. The secondary drying step involved further reducing the residual moisture content in the sample, ensuring a stable and high-quality final product. After the completion of the lyophilization process, the resulting drug-loaded NLC (BNP) was stored in a refrigerated environment to maintain its stability and prevent any potential degradation until further use. This method of processing allows for the preservation of the drug-loaded NLC's properties and can enhance its shelf-life and ease of administration.

Reconstitution of lyophilized product and its evaluation

Upon retrieving the lyophilized drug-loaded NLC (BNP) from the refrigerator, it was reconstituted with a normal saline solution to restore its original aqueous form and make it suitable for further evaluation and potential administration. To reconstitute the lyophilized product, 2.5 mg equivalent of ETR-containing BNPs was dispersed in 5 mL of normal saline. This process was facilitated with a vortex mixer, which ensured thorough mixing and uniform distribution of the NLC particles in the saline solution. The vortexing process was carried out for 1-minute to ensure optimal redispersion and to minimize any potential aggregation of the NLC particles. This reconstituted formulation was then subjected to various characterization studies to assess its physicochemical properties and performance.

Firstly, the particle size distribution of the reconstituted BNPs was analyzed, which provides information about the size and uniformity of the NLC particles in the dispersion. A narrow particle size distribution and an appropriate average particle size are desirable for optimal drug delivery performance.

Secondly, the polydispersity index (PDI) was determined. PDI is a measure of the width of the particle size distribution, with lower values indicating a more uniform distribution and better quality of the formulation. A low PDI value is preferred as it suggests a homogeneous population of particles, which can contribute to improved stability and drug release characteristics.

Lastly, the *in-vitro* drug release study was conducted to evaluate the release profile of ETR from the reconstituted BNPs under controlled conditions that simulate the physiological environment. This information is crucial for understanding the performance of the formulation in terms of drug delivery efficiency and potential therapeutic efficacy.

Preparation and evaluation of targeted nanoparticles

Mannosylated (MNP) and galactosylated (GNP) NLCs were prepared by the same method mentioned above except that stearylamine was replaced completely with an identical quantity of the synthesized conjugated lipid. The products were lyophilized as described in the case of the BNPs and reconstituted for further studies. The *in-vitro* release from the targeted particles was estimated with the protocol described earlier for evaluation of release from BNPs and the corresponding results were compared.

Cellular uptake studies in murine macrophage cell line

The study employed RAW 264.7 macrophage cell lines to examine the cellular absorption of etravirine NLCs.[14,15] Five times as many cells (five times 10^4) were sown into each well of a 48-well tissue culture plate. The cells were then incubated for the entire night at 37ºC in a carbon dioxide incubator with 5% CO2 and 95% humidity in DMEM. The medium was then aspirated, and Dulbecco's PBS was used to clean the cells. Each well received 300 µL of fresh DMEM containing the test substance at the appropriate quantities (corresponding to 25 and 50 nM of ETR as drug solution; ES, BNP, MNP, and GNP).

For the manufacture of ES, ETR was dissolved in DMSO, and the nanoparticles were then distributed again in regular saline. The media from each well was aspirated at predefined intervals (0.5, 1, 2, and 6 hours), and the cells were twice rinsed with Dulbecco's PBS. After adding 200 µL of lysis buffer (0.1% Triton X-100 in Dulbecco's PBS), the plates were left on a rocker for an hour, with 15-minute intervals of sporadic sonication for 5 minutes. Regular microscopic inspection guaranteed total lysis.

After transferring the cell lysate from each well into a new microcentrifuge tube, 200 µL of methanol was added. The supernatant was collected after centrifugation at 12,000 rpm for 10 minutes, and HPLC measured the quantities of ETR. Every test sample was examined three times. The data pertaining to the cellular absorption of ETR at a dose of 50 nM was subjected to an ANOVA analysis in order to evaluate the relevance of the findings.

***In-vitro* cytotoxicity by MTT assay in murine macrophage cell line**

The *in-vitro* cytotoxicity of various NLCs was assessed in RAW 264.7 cells.[16,17] To begin, cells were seeded in a 96-well tissue culture plate containing DMEM, following the protocol described in the uptake studies. The cells were then incubated overnight at 37ºC in a carbon dioxide incubator with 5% CO2 and 95% humidity. After the incubation period, the supernatant medium was removed from each well. Next, 200 µL of media containing the test compounds at different concentrations (ranging from 0–32 µM, with six wells per concentration) was added to the wells. The cells were further incubated for

48 hours. After this incubation period, 150 µL of DMSO was added to each well, and the contents were mixed on an orbital shaker for 15 minutes. Finally, the absorbance was measured at 570 nm, and the percentage viability was calculated with the formula:

%Viability = (Optical density of test compound/ Optical density of control) X 100

Data was subjected to one-way ANOVA to determine the significance of the results.

In-vivo biodistribution studies

Estimation of efficiency of extraction of ETR from nanoparticles trapped in tissues

The recovery of mannosylated and galactosylated nanoparticles in liver homogenates, with the drug in both solution and nanoparticle forms, was assessed. To do this, the liver tissue homogenate was pre-spiked with the analyte, and an albendazole working solution served as an internal standard, which was added to the samples post-extraction[18]. The extraction process involved the protein precipitation technique. The tissue underwent homogenization at a speed of 6000 to 8000 rpm for 10 to 15 minutes. Subsequently, the samples were centrifuged at 10,000 rpm and 20ºC for 10 minutes. The resulting supernatant was collected, and the recovery of the analyte was determined through HPLC analysis[19].

Biodistribution studies

Biodistribution studies of ETR were conducted after intravenous administration in healthy adult albino rats weighing between 180 to 200 gm. The rats were obtained from VAB Biosciences' animal house in Hyderabad, following approval from the institutional animal ethics committee and CPCSEA (IAEC/SVCP/2022/06). Throughout the study, the rats received appropriate care, food, and water and were in well-ventilated, spacious cages. The experiment involved four groups, each consisting of eighteen rats, assigned based on their body weight. Group 1 received ETR in solution (in DMSO), group 2 was given BNP, group 3 received MNP, and group 4 was treated with GNP (redispersed with normal saline) through tail vein injections. All formulations were administered at a dose equivalent to 2.5 mg/kg body weight[20].

Plasma samples were collected from the retroorbital plexus with heparinized glass capillaries at time points: 5, 30 minutes, 1, 2, 6, and 8 hours. These samples were then transferred to heparinized collection tubes. Centrifugation at 5000 X g was performed to separate the plasma. For biodistribution analysis, at specific time points of 2, 6, and 24 hours post-injection, 6 animals from each group were euthanized. Subsequently, organs such as the liver, spleen, and heart were isolated from the euthanized animals. These organs were rinsed with buffer saline and dried with filter paper. Organ homogenates were prepared before proceeding with the analysis. To determine ETR concentrations in tissue homogenates and plasma samples, the protein precipitation method was employed, followed by HPLC analysis.

RESULTS

Studies on molecular docking of mannose and galactose conjugated lipid

The study currents the predicted molecular properties of synthesized conjugated lipids. These small molecules have a molecular weight of 431.66 g/mol. ADME predictions reveal 5 to 6 hydrogen bond donors (HBD) and 6 hydrogen bond acceptors (HBA) for both lipids. The polar surface area is 102.17 A°, and the WLogP value is 3.6. Docking studies show good interactions with proteins 1JZN and 1EGG.

The galactosylated lipid exhibited a binding score of -4.3, indicating potential hydrogen bond interactions with amino acids ASP 98, GLN 96, ASP 120, ASN 119, and GLU 104 *via* hydroxyl groups of galactose. Additionally, the lipid can bond with VAL 110, ASP 93, and Leu 112 through alkyl interactions (Figure 1). The mannosylated lipid had a binding score of -3.7, featuring hydrogen bond interactions with TRP 655, LEU 669, GLY 698, SER 671, ASP 668, and GLN 760 via hydroxyl groups of mannose. The stearylamine attached to mannose can have alkyl interactions with ARG 663 and ARG 659 (Figure 2 and Table 1).

Synthesis of stearylamine-mannose (STMN) conjugate and stearylamine galactose (STGL) conjugate

The reaction between unprotected sugars, such as mono or oligosaccharides, and long-chain fatty amines, like stearylamine, in a hot alcoholic solution has been previously reported. In this process, the free anomeric hydroxyl group of mannose and galactose reacts with the amino group of stearylamine, resulting in the formation of an amine bond in secondary glycosylamine. This has been demonstrated in the case of mannose, as shown in Figure 3.

Table 1: Molecular properties and docking scores of STMN and STGL conjugates

Compound	*Mwt (g/mol)*	*Hydrogen bond donor*	*Hydrogen bond acceptor*	*Topographical surface area*	*WlogP*	*logP (Consensus)*	*Log S (SILICOS-IT)*	*BBB Permeant*	*Docking score*
Galactose linked Stearylamine PDB ID-IJZJN	431.66	5	6	102.17	3.64	4.36	-5.17 (Moderately soluble)	No	-4.3
Mannose linked Stearylamine PDB ID – 1EGG	431.66	5	6	102.17	3.64	4.36	-5.17 (Moderately soluble)	No	-3.7

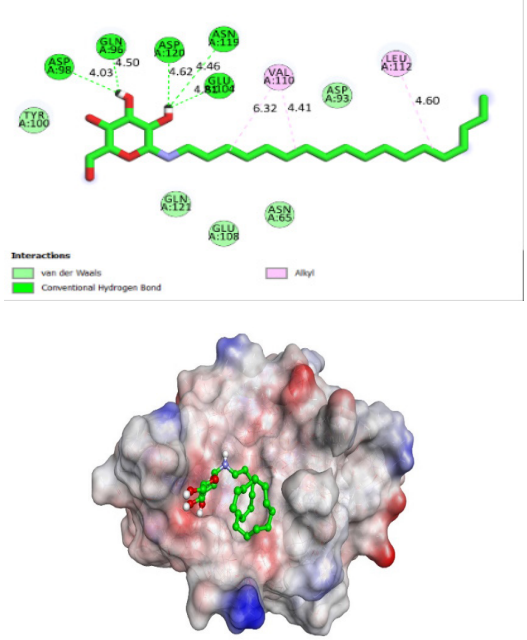

Figure 1: 2D and 3D interaction diagrams of galactosylated-stearylamine conjugated lipid with 1JZN protein

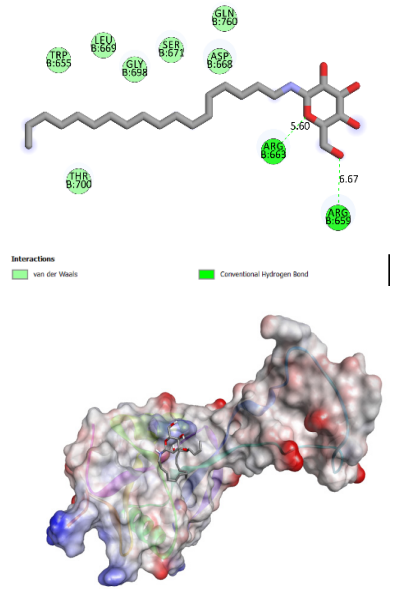

Figure 2: 2D and 3D interaction diagrams of mannosylated-stearylamine conjugated lipid with 1EGG protein

Characterization of STMN and STGL conjugates

Synthesized STMN conjugate was a brown-colored solid and could be obtained in a good yield of about 80 to 85% w/w. It showed a sharp melting point of 100ºC. Also, the reported melting point of stearylamine is 50 to 55ºC, whereas that of D-mannose is 133ºC.

STGL conjugate was obtained as a creamish-colored powder with a yield of 75 to 80% w/w and showed a melting point of 80ºC, whereas the melting point of D-galactose is 167ºC.

FTIR Spectroscopy

The Infrared (IR) spectra of STGL, STMN, and stearylamine are presented in Figures 4a, b, and c, respectively. With regard to the stearyl amine spectrum, the peaks at 3302 and 3267 cm^{-1} are ascribed to the asymmetric and symmetric N-H stretches of the stearylamine primary amine group. Furthermore, the peaks at 2918 and 2848 cm^{-1} represent the -CH_2 stretching of the long alkyl chain, and the peak at 1647 cm^{-1} is indicative of the N-H bending vibration of the primary amine.

Upon examining the FTIR studies of the conjugated products, it is evident that the -CH2 stretching peaks are preserved, and the peaks related to the N-H stretch are also clearly discernible, albeit broadened, potentially due to overlap with the O-H stretch from the sugars. Notably, the peak corresponding to the N-H bend at 1647 cm^{-1} is absent, indicating the binding of sugars at the primary amine group and successful conjugation.

H^1 NMR Spectroscopy of STMN and STGL conjugates

Figures 5a and b show the chemical shift of synthesized STMN and STGL conjugates, which shows the long alkyl chain proton

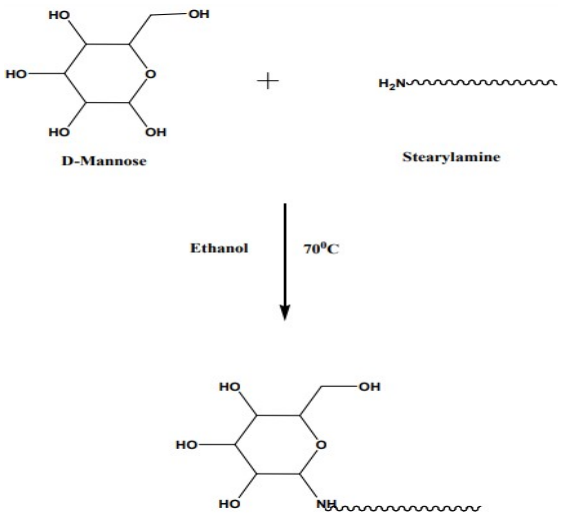

Figure 3: Structure of the synthesized conjugate (STMN)

at a delta symbol 1.22 ppm and small intensity of NH- proton at a delta 1.36 ppm. Also, the protons seen further downfield of about 3 ppm can be attributed to those from the sugars, indicating a successful reaction.

Mass Spectroscopy

The theoretical molecular weight of STMN and STGL conjugates can be approximately calculated as 431.655. The mass spectra of STMN and STGL are displayed in Figures 6a and b, respectively. In both cases, a molecular peak at m/z = 432, corresponding to the molecular ion peak, was noted in positive electrospray ionization (ESI) mode. This observation confirms the formation of the conjugates with a molecular formula of C24H49NO5. Other peaks at m/z = 270.3, 242.3, 243.3, etc., may correspond to various fragments.

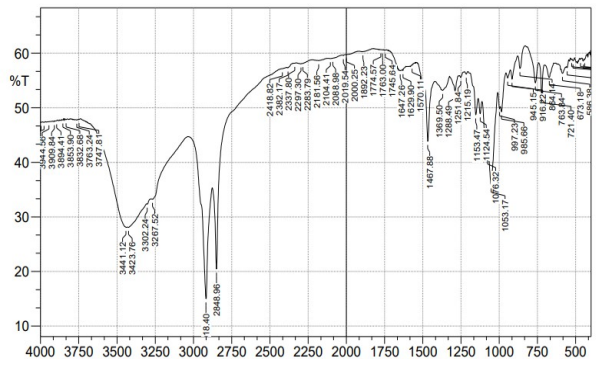

Figure 4a: FTIR spectroscopy of stearylamine

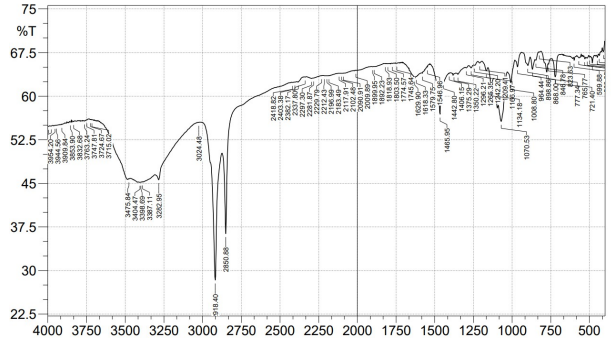

Figure 4b: FTIR spectroscopy of stearylamine-mannose conjugated lipid (STMN)

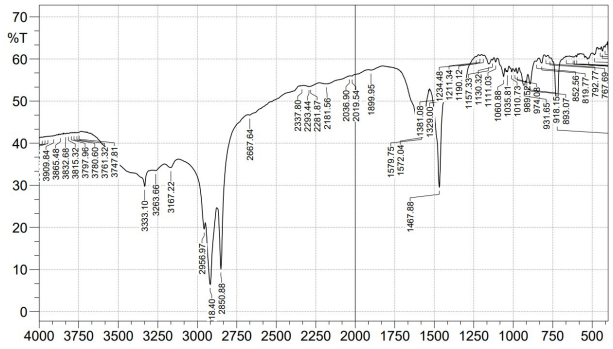

Figure 4c: FTIR spectroscopy of stearylamine-galactose conjugated lipid (STGL)

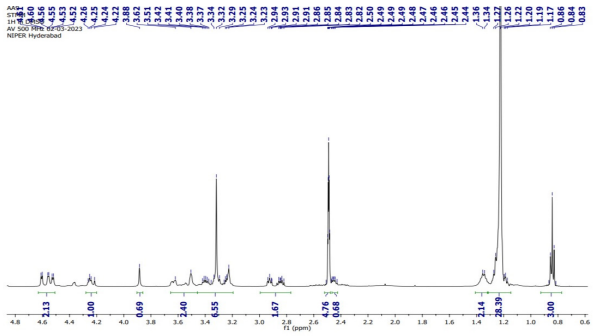

Figure 5a: ^{1}H-NMR of STMN conjugate

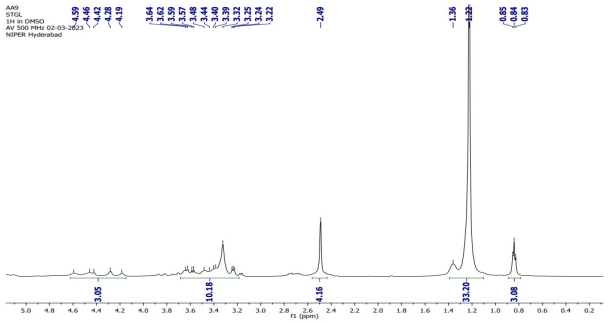

Figure 5b: ^{1}H-NMR of STGL conjugate

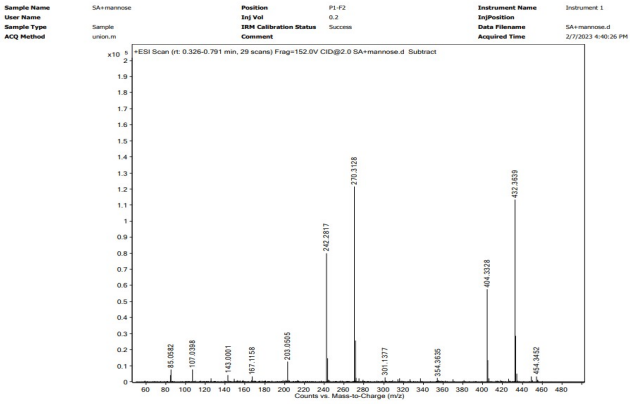

Figure 6a: Mass spectroscopy of STMN conjugate

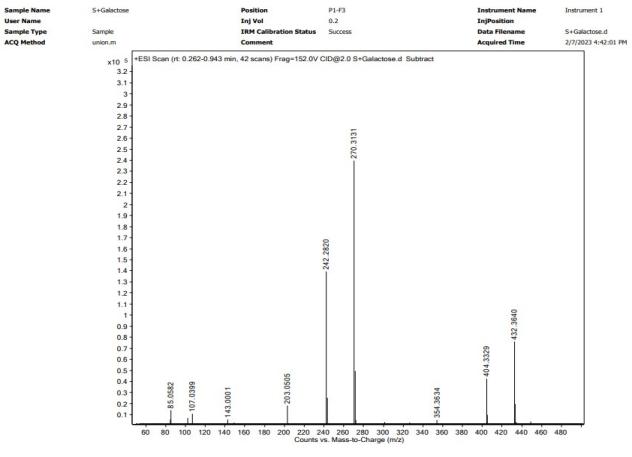

Figure 6b: Mass spectroscopy of STGL conjugate

Preparation and characterization of non-targeted nanoparticles

The laboratory-friendly emulsion solvent evaporation method was used to prepare the ETR-loaded NLC.

Particle size and zeta potential

The Z-average particle size of the prepared NLC was determined to be 261.6 nm, with a polydispersity Index (PDI) of 0.374, as demonstrated in Figure 7. The PDI value of 0.374 suggests that the nanoparticles' size distribution was relatively narrow. The zeta potential of the optimized formulation was measured at -10.1 mV, as shown in Figure 8.

Scanning Electron Microscopy

The SEM image of the NLCs seen in Figure 9 also reflects a similar finding and the size of the particles can be adjudged to

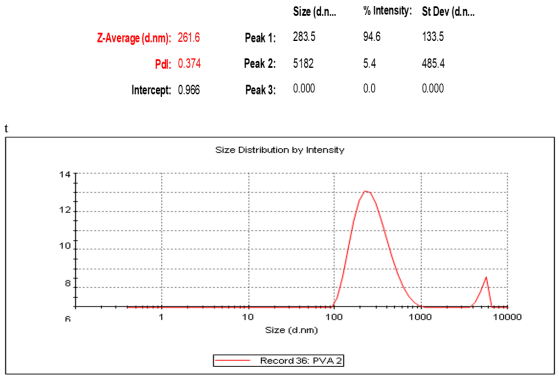

Figure 7: Average particle size of NLC formulation

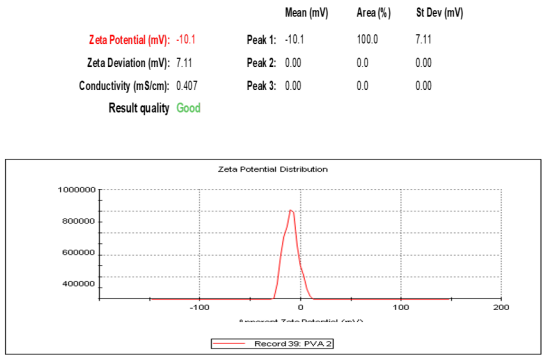

Figure 8: Zeta potential of etravirine-loaded NLC formulation

be about 250 nm. The nanoparticles appear in loose aggregates and the uniformity in size is also apparent.

Entrapment efficiency

The entrapment efficiency of all the formulations was found to be between 97.45 to 99.00%, so drug loss during preparation was minimal.

In-vitro drug release studies

In-vitro release of ETR from the BNPs is given in Figure 10. As seen, a low burst followed by a sustained release of ETR was obtained from the nanoparticles and nearly 60% of the entrapped ETR was released over the 24 hours study period.

Lyophilization and evaluation of the product after reconstitution

The lyophilization process, performed in the presence of mannitol as a cryoprotectant, proved successful for the dispersion. Following lyophilization, the products were reconstituted with a normal saline solution. Upon redispersion in an aqueous medium, the product exhibited a Z-average size of 287.5 nm and a PDI of 0.432, as per Figure 11. Although these values were slightly higher than the size and PDI of the sample before lyophilization, they remained within acceptable limits. Notably, the enhancement in size did not adversely impact the release from the nanostructured lipid carriers (NLCs), as demonstrated in Figure.

Preparation and evaluation of targeted nanoparticles

To create targeted nanoparticles, the same procedure as the non-targeted ones can be employed, with the only

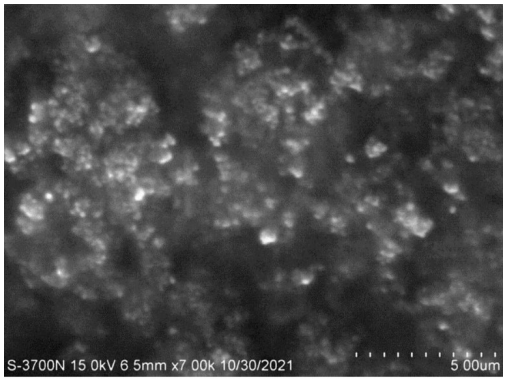

Figure 9: SEM image of NLC formulation

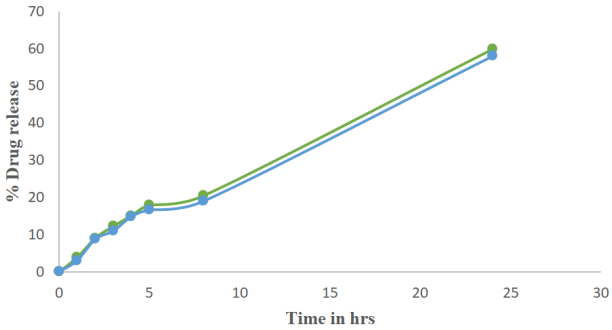

Figure 10: *In-vitro* release studies of BNP (non-lyophilized and lyophilized products) BNP non-lyophilized BNP lyophilized

modification being the substitution of stearylamine with sugar-conjugated lipids. The mannosylated nanoparticles (MNPs) and galactosylated nanoparticles (GNPs) in their lyophilized form, upon reconstitution and release studies, displayed a release profile similar to that of the non-mannosylated/non-galactosylated nanoparticles (BNPs), as depicted in Figure 12. This suggests that the replacement of the lipid did not alter any of the other physicochemical attributes of the nanoparticles.

Cellular uptake studies

In order to investigate drug uptake in macrophage cells, a murine macrophage cell line (RAW 264.7) was employed. The cells were exposed to 25 and 50 nM concentrations of ES (solution), BNP, MNP, and GNP for durations of 0.5, 1, 2, and 6 hours. As per Figures 13a and b, the solution exhibited a rapid cellular uptake compared to nanoparticles at every time point and concentration. The uptake of ETR from nanoparticles was comparatively slow. Notably, there was a significant variation in cellular uptake between BNP, MNP, and GNP.

At 25 nM concentration of ETR, only MNP facilitated a detectable ETR entry into cells after 6 hrs, while uptake from GNP and BNP remained insignificant. At 50 nM, the cellular uptake of MNP enhanced consistently over time, and by 6 hrs, MNP uptake surpassed that of BNP, GNP, and the ETR solution. A two-way ANOVA analysis demonstrated a significant difference (p <0.05) in the extent of cellular uptake among the various groups at the 50 nM concentration level.

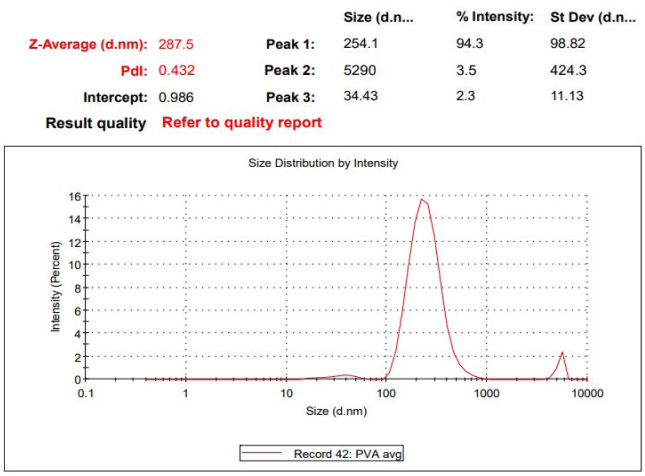

Figure 11: Average particle size of lyophilized NLC formulation

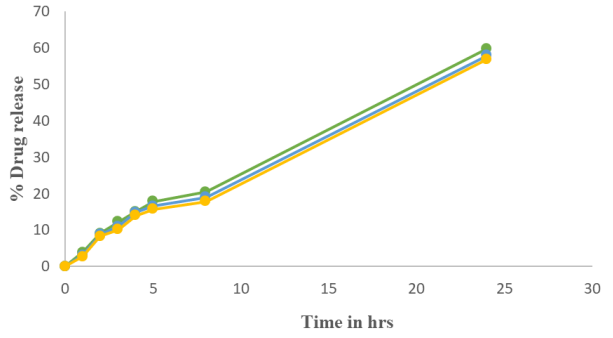

Figure 12: *In-vitro* release studies of BNP (lyophilized and targeted nanoparticles MNP and GNP) BNP lyophilized ■ MNP lyophilized ■ GNP lyophilized

In-vitro cytotoxicity study by MTT assay in RAW 264.7 cell line

Using mouse macrophage cells (RAW 264.7), an MTT assay was used to evaluate the relative cytotoxicity of mannose-conjugated nanoparticles (MNPs) and galactose-conjugated nanoparticles (GNPs) of ETR. The purpose of the study was to ascertain the viability of RAW 264.7 cells in both solution and nanoparticle form when exposed to various ETR concentrations (0, 2, 4, 8, 16, and 32 µM). Figure 14 displays the current results. ETR demonstrated concentration-dependent cytotoxicity. Interestingly, GNPs exhibited very minimal cytotoxicity even at the highest concentration tested, indicating that they were less deadly than non-targeted nanoparticles. However, MNPs showed cytotoxic effects, making them more dangerous than ETR alone at higher dosages. A One-way ANOVA statistical analysis confirmed that there was a significant difference in cytotoxicity between the groups at 8, 16, and 32 µM (p <0.05).

In-vivo biodistribution studies

Estimation of efficiency of extraction of ETR from nanoparticles trapped in tissues.

Extraction recovery, a vital parameter in analytical procedures, quantifies the percentage of an analyte retrieved after extraction and sample processing. In the context of nanoparticles in tissues, extraction recovery studies demonstrated that the developed method effectively recovered all free etravirine and a substantial portion of etravirine in tissue as nanoparticles.

Table 2 highlights the recovery of ETR in various forms. When ETR was introduced as a solution into liver tissue, the recovery was 100%. Additionally, ETR in the form of BNP, MNP, and GNP also showed good recovery rates, indicating the method's success in retrieving and analyzing these nanoparticle forms.

Biodistribution Studies

The research focused on evaluating the drug concentrations in various organs, particularly those with high lectin receptor

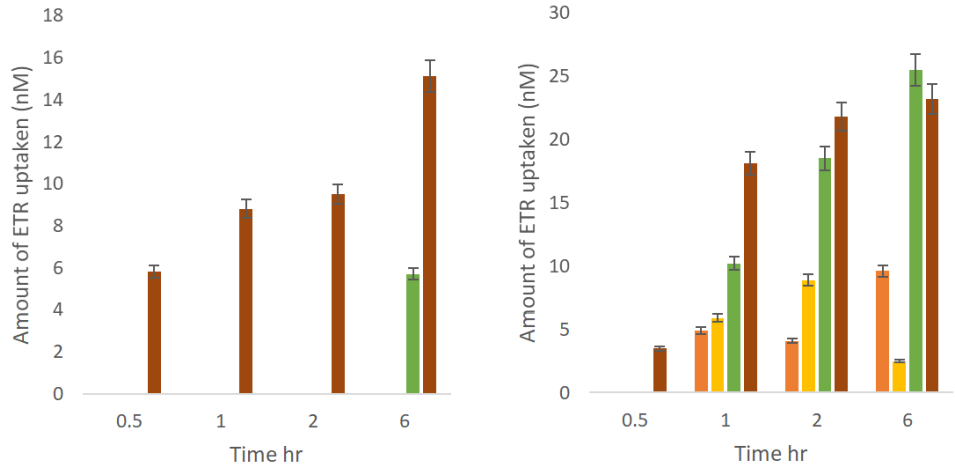

Figure 13a & 13b: Uptake of BNP, MNP, GNP and ES at a) 25 nM and b) 50 nM by RAW 264.7 cells. ■ BNP ■ GNP ■ MNP ■ ES. When analysed by two-way ANOVA a significant difference in the extent of cellular uptake between the different groups was obtained at the 50 nM concentration level ($p < 0.05$).

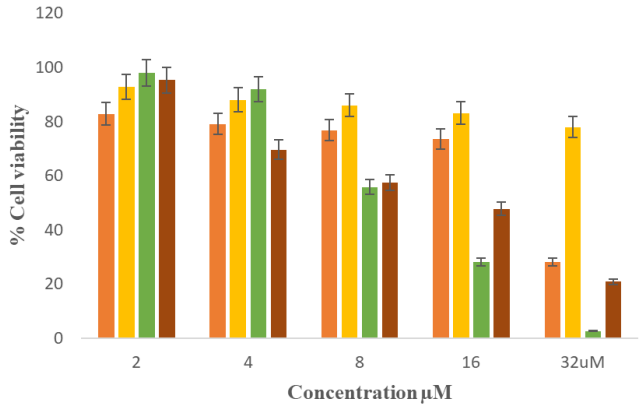

Figure 14: In-vitro cytotoxicity assessment of BNP, MNP, GNP and ES to RAW 264.7 cells studied by MTT assay. ■ BNP ■ GNP ■ MNP ■ ES. Data values when analysed by one way ANOVA significant difference was seen between different groups at 8, 16 and 32 µM ($p < 0.05$).

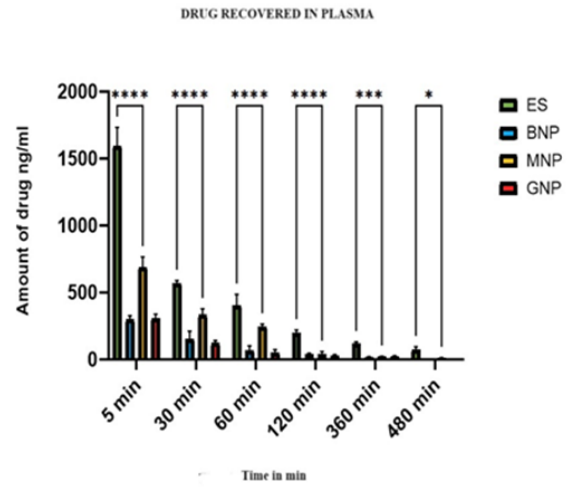

Figure 15a: Amount of ETR recovered in plasma

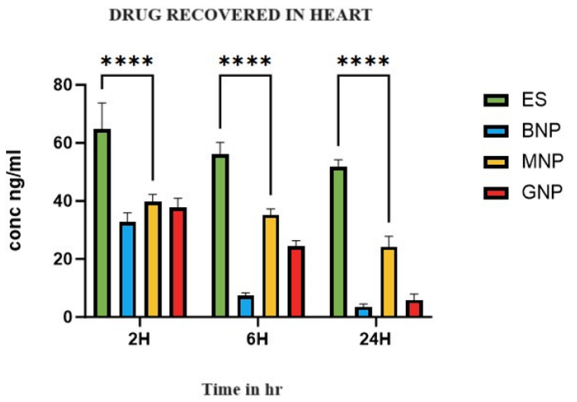

Figure 15b: Amount of ETR recovered in heart

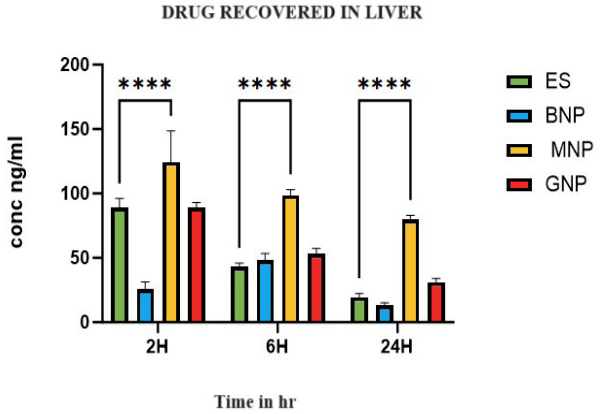

Figure 15c: Amount of ETR recovered in liver

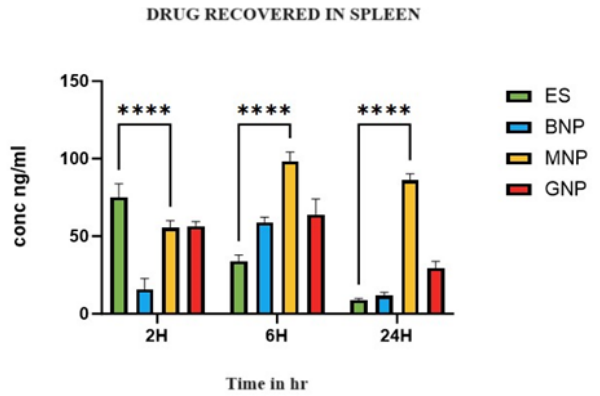

Figure 15d: Amount of ETR recovered in spleen

presence. Graphs 15a, b, c, d display the drug levels in blood plasma and the liver, spleen, and heart at distinct time intervals (2, 6, and 24 hours) following the intravenous tail vein administration of ES, BNPs, GNPs, and MNPs, as well as control nanoparticles, mannosylated nanoparticles, and galactosylated nanoparticles at a 2.5 mg/kg equivalent therapeutic response (ETR) dosage.

Rats were given etravirine solution (ES) and etravirine-loaded NLCs BNP, MNP, and GNP (2.5 mg/kg) intravenously for 2, 6, and 24 hours, respectively. (**** indicates $p < 0.0001$, a significant statistical difference using a two-way ANOVA and the Tukey-Krammer test compared to plain ES.

In the aforementioned study, a consistent pattern was noticed where the ETR levels in plasma remained detectable for up to 8 hours when administered as a solution, contrasting the rapid clearance observed in the nanoparticle forms. This rapid distribution from the vascular compartment was more evident in the nanoparticle-based ETR formulations. Interestingly, the drug solution form allowed for a more extensive reach of ETR in the heart compared to the nanoparticle-based formulations.

Moreover, MNPs enabled higher concentrations of ETR in the liver and spleen, which are macrophagic tissues, as compared to the solution, BNPs, and GNPs. A two-way Analysis of Variance substantiated these findings (ANOVA) combined with a Tukey-Kramer multiple comparisons test, establishing a highly significant threshold at $p < 0.0001$ (denoted by "****"). This stringent statistical methodology fortifies the credibility and validity of the results obtained in the study.

Table 2: Extraction recovery of ETR from nanoparticles in tissue

Concentration (µg/mL)	*Etravirine*	*IS*	*Ratio*	*Known concentration (µg/ml)*	*%recovery*
10	3147375	170403	18.5	10.0	100
20	6352971	172888	36.7	20.0	100
	BNP (non-targeted NLC)				
10	3187069	184859	17.2	9.31	93.3
20	6086416	184485	33.0	8.0	89.8
	GNP (Galactosylated NLC)				
10	2599113	192381	13.5	7.3	73.1
20	5650261	193621	29.2	15.9	79.4
	MNP (Mannosylated NLC)				
10	3429174	208686	16.4	8.9	89.0
20	6696601	200260	33.4	18.2	91.0

DISCUSSION

The objective of the current work was to study the effectiveness of mannosylated and galactosylated lipid nanoparticles for targeting ETR to the macrophagic viral reservoirs. Here, stearylamine was chosen as the lipid for tagging with the monosaccharides. Stearylamine has been used in liposomal drug delivery systems to impart a positive charge[21] as well as in lipidic systems to enable the attachment of targeting ligands, including mannose[22]. Hence, in the current work too, stearylamine was included in the lipid matrix of the nanoparticles to provide amine terminated functionality for the attachment of the targeting ligands. Prior to synthesis, a docking study was used to analyze the potential of the ligands for interaction with the respective lectin receptors and the results.

It can be concluded from the Molinspiration values and docking studies that the conjugated lipids have good binding characteristics towards the respective protein receptors, which could help in favoring interactions between the ligand and the target receptor,[23] which, in turn, may be indicative of the ability of the cells bearing these receptors for uptake of nanoparticles decorated with the ligands. Based on these findings, both mannosylated (STMN) and galactosylated (STGL) stearylamine derivatives were synthesized for further evaluation.

STMN and STGL conjugates synthesized were evaluated for their physical and spectral properties. The melting points of STMN and STGL are different from that of the stearylamine and also that of the sugars, indicative of the successful formation of the respective conjugates. Likewise, FTIR, NMR and mass spectroscopic data indicate successful conjugation. The synthesized sugar derivatives of stearylamine were then used to replace stearylamine on a weight-by-weight basis during the preparation of the targeted nanoparticles.

Initially, solvent emulsification and evaporation were used to create the ETR-loaded non targeted NLCs (BNP). The selection of stearylamine and glyceryl monostearate as solid lipids and Capryol 90 as a liquid lipid was based on their solubility of etravirine and their biocompatibility. Dichloromethane was also utilized as the solvent because of its volatility and the fact that all of the components showed sufficient solubility it.

The proportion of lipids used for the entrapment of etravirine and the concentration of polyvinyl alcohol as a stabilizer in the preparation medium was intended to yield nanoparticles with a low burst, sustained release over a 24-hour period and a target size of 250 nm considered suitable for macrophage uptake.

The produced nanoparticle's zeta potential and particle size were assessed. The generated NLC's average particle size was 261.6 nm, which is said to be the perfect size for targeting organs, including the liver, spleen, and other tissues linked to macrophages[24]. A zeta potential greater than ± 30 mV is thought to be a reliable sign of the nanoparticle dispersion stability. Mannitol was added to the suspension during lyophilization as a cryoprotectant because the zeta potential of the nanoparticles produced here was recorded at -10.1 mV. The suspension was meant to be replenished during administration. The particles wouldn't aggregate while being stored if they were freeze-dried. The entrapment efficiency of all the nanoparticles indicated a high proportion of the drug molecules effectively incorporated into the NLCs. This is attributed to the poor solubility of ETR in the aqueous preparation medium and good solubility in the selected lipidic mixture. From the release studies, it is noteworthy that there was no significant burst release of ETR from the particles, which is intended to ensure that no premature release of the drug payload occurs prior to reaching the target macrophagic cells. Further, although the hydrodynamic particle size and the polydispersity index of the particles redispersed post-lyophilization, were found to be slightly more than the initial values, the release of ETR from the nanoparticles, which was considered a key performance attribute, remained unaltered. Similarly, replacing the stearylamine with either sugar-conjugated stearylamine also did not impact the release from the nanoparticles and they were considered suitable for uptake studies in cell lines and also *in-vivo* biodistribution studies.

To assess cytotoxicity and absorption *in-vitro*, RAW 264.7, a murine macrophage cell line was employed. These cells, which are produced from a cell line transformed by the Abelson leukemia virus and derived from BALB/c mice, resemble monocytes and macrophages. RAW 264.7 cells are a suitable macrophage model because of their capacity for phagocytosis and pinocytosis.[25] They express lectin receptors, such as mannose and galactose, on their cell surface, enabling the assessment of nanoparticle targeting potential with NLCs.[26,27] (nanostructured lipid carriers). Numerous studies have confirmed the suitability of this cell line for such investigations.

In the study, free ETR demonstrated concentration- and time-dependent uptake, which can be attributed to its small molecular size and ease of access to cells through transcellular transport. In contrast, nanoparticle uptake occurred at a slower pace, suggesting a distinct mechanism. Although galactosylation did not offer any advantages over non-targeted nanoparticles, mannosylated particles exhibited enhanced uptake, particularly at higher concentrations. This finding aligns with previous reports.[28] The heightened cellular uptake of mannosylated NLCs (nanostructured lipid carriers) by RAW 264.7 cells can be attributed to the predominance of mannosyl receptors on macrophage cell surfaces, which play a role in phagocytosis.[29] Consequently, mannosylated NLCs were phagocytosed to a greater extent. The lower efficacy of galactosylation compared to mannosylation in promoting nanoparticle uptake by RAW 264.7 cells has also been observed in studies involving poly(lactide-co-glycolide) nanoparticles decorated with various carbohydrate moieties designed for macrophage gene delivery.[30]

The results also, however, indicate the possibility of a lag time before internalization of the mannosylated nanoparticles. Since the particles were engineered to release the drug with minimal burst and do so after a lag time of 2 hours, this delay may prevent drug loss prior to internalization by the macrophages.

The *in-vitro* cytotoxicity findings align with the uptake studies, suggesting that the heightened toxicity of MNPs (magnetic nanoparticles) might be attributed to their enhanced uptake via mannose receptors on macrophages. Conversely, GNPs (gold nanoparticles) demonstrated no uptake and were non-toxic to RAW 264.7 cells. Likewise, other studies involving lipidic particles have reported enhanced toxicity of the encapsulated drug in correlation with improved uptake.[30] It is noteworthy that the EC50 of ETR (Etravirine) is reportedly less than 5 Nm[31] in most resistant HIV strains. The concentrations of ETR used in our cytotoxicity assessments were approximately 1000-fold higher, aiming to evaluate the relative toxicity of the formulations.

Since the drug was entrapped in the lipidic nanoparticles prior to the biodistribution studies, it was thought essential to validate the method of extraction of ETR and to ensure that the drug was extracted from any lipidic particles that may have partitioned into the tissue from blood. The results of the experiment validated the suitability of the extraction process. Etravirine, clinically administered via oral route with a typical adult dose of 200 mg, exhibits poor oral bioavailability. This dose results in a C_{max} (maximum concentration) within the range of 100 to 400 ng/mL.[32] In our studies, administration was through the IV (intravenous) route, and the dosage was chosen based on previous reports. Following ETR administration with etravirine suspension (ES), plasma concentration peaked nearly double at the 5-minute mark and remained elevated compared to the levels achieved with nanoparticles. This can be attributed to ETR's high protein binding efficiency of 99%, which prolongs its presence in the blood. *In-vitro* studies demonstrate that the agent binds to albumin (HSA) with 99.6% efficiency and 97.7% to alpha-1-acid glycoprotein (AAG).[33-37]

In contrast, the nanoparticles containing etravirine were rapidly redistributed and irrespective of whether the nanoparticles were untagged or tagged with mannose/galactose, etravirine levels in plasma declined rapidly, a clear indicator that the nanoparticles successfully altered the biodistribution of the drug. Also, while etravirine was found in greater levels in the heart, a non-target tissue, less amount of etravirine could be detected in cardiac tissue when administered as nanoparticles. More significantly, in the case of target organs like the spleen and liver, etravirine as a solution showed high levels at 2 hours but declined rapidly. In contrast, etravirine administered as nanoparticles was resident in these organs for much longer, with appreciable levels detected even at the end of 24 hours. The reasons could be the prolonged retention of the nanoparticles in these organs and the gradual release of ETR from the particles. Among the nanoparticles investigated, however, the mannose-tagged particles resulted in significantly higher levels in the target organs, which possibly indicated greater levels of cellular uptake, a conclusion fortified by the results of the uptake studies in RAW 264.7 cells reported here. The results lead to the conclusion that mannosylated nanoparticles are successful in targeting the antiviral drug to the macrophagic tissues while sparing the non-macrophagic tissues.

CONCLUSION

Macrophages serve as the primary constituent cells within the mononuclear phagocyte system, and they are distributed across vital organs such as the liver, lungs, spleen, lymph nodes, and the gastrointestinal tract. In the context of our recent investigations, macrophages' mannose and galactose receptors have been strategically utilized to target nanoparticle-bearing ligands, thereby enhancing their specific interaction with these immune cells. The results indicate that nanoparticles, targeted or otherwise can alter the biodistribution of the anti-HIV drug. In addition, successful uptake into the target tissue may be achieved as in the case of mannosylated nanoparticles prepared in the current study and thus, an enhancement in efficacy of the formulation can also be achieved. However, the choice of the sugar used as the targeting ligand may be critical to the success of the system.

ACKNOWLEDGMENTS

The authors express their gratitude to Hetero Pharmaceuticals Ltd., Hyderabad, for generously offering etravirine as a complimentary sample and to Gattefosse, Mumbai, for providing us with Capryol 90. We are indebted to Sri Venkateshwara College of Pharmacy, Hyderabad, and Gokaraju Rangaraju College of Pharmacy, Hyderabad, for their unwavering support and providing the essential resources required to conduct this research successfully. I would also like to thank Acubiosys Pvt Ltd for helping me in conducting the study.

REFERENCES

1. Meltzer MS, Skillman DR, Gomatos PJ, Kalter DC, Gendelman HC. Role of mononuclear phagocytosis in the pathogenesis of human immunodeficiency virus infection. Annu Rev Immunol. 1990; 8:169-194.
2. Oussoren C, Magnani M, Fraternale A, Casabianca A, Chiarantini L, Ingebrigsten R, Underberg WJM, Strome G. Liposomes as carrier of the antiretroviral agent dideoxycytidine-5'-triphosphate. Int J Pharm. 1999; 180: 261-270.
3. Schafer V, Briesen HV, Rubsamen-Waigmann H, Steffan AM, Royer C, Kreuter J. Phagocytosis and degradation of human serum albumin microspheres and nanoparticles in human macrophages. J Microencapsul. 1994; 11: 261-269.
4. Cui Z, Hsu CH, Mumper RJ. Physical characterization and macrophage cell uptake of mannan-coated nanoparticles. Drug Dev Ind Pharm. 2003; 29: 689-700.
5. Kaur A, Jain S, Ashok K. Mannan -coated gelatin nanoparticles for sustained and targeted delivery of didanosine: *In-vitro* and *in-vivo* evaluation. Acta Pharm. 2008; 58: 61-74.
6. Wadhwa MS, Rice KG. Receptor mediated glycol-targeting. J. Drug Target. 2003;11: 255-268.
7. Shao J, Ma JK. Characterization of mannosyl phospholipid liposome system for drug targeting to alveolar macrophages. J Drug Deliv Target Ther Agents.1997; 4: 43-48.
8. Adams J, Patel N, Mankaryous N, Tadros M, Miller CD. Non-nucleoside reverse transcriptase inhibitor resistance and the role of the second-generation agents. Ann Pharmacother. 2010; 44: 157-165.
9. Zeeshan M, Ali H, Ain QU, Mukhtar M, Gulch R, Sarwar A, Khan S. A holistic QBD approach to design galactose conjugated PLGA polymer and nanoparticles to catch macrophages during intestinal inflammation. Mater Sci Eng. 2021; 112183: 1-18.
10. Lockhoff O, Stadler P. Synthesis of glycosamides as glycolipid analogs. Carbohydrate research. 1998; 314(1): 13-24.
11. Huang Y, Hu Lu, Huang S, Xu W, Wan J, Wang D, Zheng G, Xia Z. Curcumin loaded galactosylated BSA nanoparticles as targeted drug delivery carriers inhibit hepatocellular carcinoma cell proliferation and migration. Int J Nanomedicine. 2018;13: 8309-8323.
12. Shah J, Patel S, Srinivas B, Rajashree H. Formulation optimization, characterization and *in-vivo* anti-cancer activity of curcumin loaded nanostructured lipid carriers. Int. J. Curr. Pharm Rev. Res. 2022; 14(1): 31-43.
13. Siow CRS, Wan Sia Heng P, Chan LW. Application of freeze drying in the development of oral drug delivery systems. Expert opin Drug Delivery. 2016; 13(11):1595-1608.
14. Chang H, Yhee JY, You GH, Ryu JH, Choi Y, Na JH, Park JH, Lee KH, Choi K, Kim K, Kwon IC. Predicting the *in-vivo* accumulation of nanoparticles in tumour based on *in-vitro* macrophage uptake and circulation in zebrafish. JCR. 2016; 1-9.
15. Gyati SA, Abhay A, Dharam Veer K, Suresh Prasad V. Mannosylated Chitosan nanoparticles for delivery of antisense oligonucleotides for macrophage targeting. Bio Med Research International 2014; 1-17.
16. Sant S, Poulin S, Hildgen P. Effect of polymer architecture on surface properties, plasma protein adsorption and cellular interactions of pegylated nanoparticles. Inc J Biomed Mater Res. 2008; 87: 885-895.
17. Pinheiro M, Ribeiro R, Vieira A, Andrade F, Reis S. Design of a nanostructured lipid carrier intended to improve the treatment of tuberculosis. Drug Des Devel Ther 2016;10: 2467-2475.
18. Yuan L, Ma L, Dillon L, Fancher RM, Sun H, Zhu M, Mckeeman LL, Aubry AF, Qin C. Investigation of the "true" extraction recovery of analytes from multiple types of tissues and its impact on tissue bioanalysis with two model compounds. Analytica Chimica Acta. 2016; 1-10.
19. Shriram BK, Devhare LD, Mehrotra A, Deokar SS, Singh SP. Formulation and Evaluation of Mosquito Repellent Stick. International Journal of Drug Delivery Technology. 2023;13(4):1283-1286.
20. John J, Liang D. Oral liquid formulation of etravirine for enhanced bioavailability. J Bioequivalence and Bioavailab. 2014; 6(2): 46-52.
21. He K, Liu J, Gao Y. Preparation and Evaluation of Stearylamine-Bearing Pemetrexed Disodium-Loaded Cationic Liposomes *In-vitro* **and** *In-vivo*. AAPS Pharm Sci Tech. 2020; 21(5): 193: 1-10.
22. Gupta MK, Sansare V, Shrivastava B, Jadhav S, Gurav P. Fabrication and evaluation of mannose decorated curcumin loaded nanostructured lipid carriers for hepatocyte targeting: *In-vivo* hepatoprotective activity in Wistar rats. Pharmacol Drug Discov. 2022; 3:100083.
23. Pingili D, Prasad SV, Raghavendra NM. Discovery of Novel 1,2,4-Oxadiazolyl Triazole Hybrids as B-Raf Inhibitors for the treatment of Melanoma. Chemistry Select. 2022; 7(47).
24. Jindal AB, Bachhav SS, Devarajan PV. In-situ hybrid nano drug delivery system of antiretroviral drug for simultaneous targeting to multiple viral reservoirs: an *in-vivo* proof of concept. Int J Pharm. 2017; 521: 196-203.
25. Taciak B, Bialasek M, Braniewska A, Sas Z, Sawicka P, Kiraga L. Rygiel T, Kroi M. Evaluation of phenotypic and functional stability of RAW 264.7 cell line through serial passages. PLOS One. 2018;13(6): 1-13.
26. Devhare LD and Gokhale N. Antioxidant and Antiulcer Property of Different Solvent Extracts of Cassia Tora Linn. Research Journal of Pharmacy and Technology. 2022;15(3);1109-1113..
27. Viswanathan V, Mehta H, Pharande R, Bannalikar A, Gupta P, Gupta U, Mukne A. Mannosylated gelatin nanoparticles of licorice for use in tuberculosis: Formulation, *in-vitro* evaluation, *in-vitro* cell uptake, *in-vivo* pharmacokinetics and *in-vivo* anti-tubercular efficacy. J Drug Deliv Sci Technol. 2018; 45(1): 255-263.
28. Chen Q, Gao M, Li Z, Xiao Y, Bai X, Oti K, Yiadom B, Xu X, Zhang XQ. Biodegradable nanoparticles decorated with different carbohydrates for efficient macrophage-targeted gene therapy. JCR. 2020; 323:179-190.
29. Dossou AS, Mantsch ME, Sabnis N, Berg RE, Fudala R, Lacko AG. Mannose-functionalization of reconstituted high-density

lipoprotein nanoparticles improves payload delivery and enhances M2-M1 phenotype reprogramming of RAW 264.7 macrophages polarized by B16-F10 melanoma cells. Front Drug Deliv. 2023;(3): 1-20.
30. Rojekar S, Abadi LF, Mahajan K, Kulkarni S, Vavia PR. Multi-organ targeting of HIV-1 viral reservoirs with etravirine loaded nanostructured lipid carrier: An *in-vivo* proof of concept. Eur J Pham Sci. 2021;154: 1-18.
31. Grennan T, Walmsley S. Etravirine for HIV-1: Addressing the limitations of the Nonnucleoside Reverse Transcriptase Inhibitor Class. Journal of the International Association of Physicians in AIDS Care. 2009; 8(6): 354-363.
32. Seng AT, MacArthur RD. Profile of etravirine for the treatment of HIV infection. Therapeutics and clinical risk management. 2010; 6:49-58.
33. Havens JP, Podany AT, Scarsi KK, Fletcher CV. Clinical Pharmacokinetics and Pharmacodynamics of Etravirine: An updated review. Clin Pharmacokinet. 2020; 59(2):137-154.
34. Sonule M, Devhare LD, Babu MN, Gunjal SD, Varalaxmi S. Microemulgel-based Hydrogel of Diclofenac Sodium using Lipidium sativum as a Gelling Agent. International Journal of Drug Delivery Technology. 2023;13(4):1235-1239.
35. Shriram BK, Devhare LD, Mehrotra A, Deokar SS, Singh SP. Formulation and Evaluation of Mosquito Repellent Stick. International Journal of Drug Delivery Technology. 2023;13(4):1283-1286.
36. Choudhary RK, Beeraka S, Sarkar BK, Dharmamoorthy G, Devhare L. Optimizing Verapamil Hydrochloride In-situ Delivery: A Strategic Formulation Approach using Box-Behnken Design for Enhanced Performance and Comprehensive Evaluation of Formulation Parameters. International Journal of Drug Delivery Technology. 2024;14(1):61-70.
37. Kumar KK, Kiran V, Choudhary RK, Devhare LD, Gunjal SD. Design Development and Characterization of Nicardipine Solid Lipid Nano-Particulars. International Journal of Drug Delivery Technology. 2024;14(1):71-78.